

Journal of Intelligent Material Systems and Structures

<http://jim.sagepub.com/>

Delamination detection in composite beams using pure Lamb mode generated by air-coupled ultrasonic transducer

Zenghua Liu, Hongtao Yu, Cunfu He and Bin Wu

Journal of Intelligent Material Systems and Structures 2014 25: 541 originally published online 3 July 2013

DOI: 10.1177/1045389X13493339

The online version of this article can be found at:

<http://jim.sagepub.com/content/25/5/541>

Published by:



<http://www.sagepublications.com>

Additional services and information for *Journal of Intelligent Material Systems and Structures* can be found at:

Email Alerts: <http://jim.sagepub.com/cgi/alerts>

Subscriptions: <http://jim.sagepub.com/subscriptions>

Reprints: <http://www.sagepub.com/journalsReprints.nav>

Permissions: <http://www.sagepub.com/journalsPermissions.nav>

Citations: <http://jim.sagepub.com/content/25/5/541.refs.html>

>> [Version of Record](#) - Feb 27, 2014

[OnlineFirst Version of Record](#) - Jul 3, 2013

[What is This?](#)

Delamination detection in composite beams using pure Lamb mode generated by air-coupled ultrasonic transducer

Zenghua Liu, Hongtao Yu, Cunfu He and Bin Wu

Abstract

The interaction of Lamb wave A_0 mode with delamination and delamination detection in 16-ply carbon fiber–reinforced epoxy composite beams are investigated through three-dimensional finite element simulation and experimental studies in this article. Wave propagation in composite beams with delamination with different lengths and located at different interfaces are investigated in finite element simulations, and some unique mechanisms of interaction between A_0 mode and delamination are revealed in detail. Experimental results obtained with air-coupled ultrasonic transducers are well in accordance with finite element simulation results. In an experimental study, an air-coupled ultrasonic transducer is oriented at a coincidence angle such that it generates a pure fundamental antisymmetric Lamb wave mode A_0 for delamination detection in laminated composite beams. The receiving transducer can be oriented either to detect the transmitted wave propagating in the same direction as incident wave or to detect the reflected wave in contrast to incident wave. The location and size of delamination can be evaluated quantitatively using the time-of-flight of reflected wave from both ends of the delamination.

Keywords

Delamination detection, composite beam, Lamb wave mode, air-coupled ultrasonic transducer, three-dimensional finite element simulation

Introduction

Composite materials are becoming the primary structural components in many industries such as aerospace, civil, and energy engineering because of their attractive properties of high strength, high stiffness, and low weight. Delamination is the most common damage in composite materials during manufacturing and service processes (Islam and Craig, 1994). To ensure the integrity and reliability of the materials, viable damage prognosis and structural health monitoring methods (Farrar and Lieven, 2007), for example, Lamb wave–based techniques (Cawley and Alleyne, 1996; Giurgiutiu, 2005; Lee et al., 2011; Rizzo et al., 2010) and electromechanical impedance techniques (Mascarenas et al., 2010; Park et al., 2003), are needed. For the testing of composite laminates, Lamb wave–based technique is a good choice because that Lamb waves are guided by geometrical boundaries to propagate long distances even in materials with a high attenuation ratio, and various Lamb modes can interrogate the entire thickness of the laminate (Guo and Cawley, 1994; Su et al., 2006;

Wilcox et al., 2001). In addition, there are many guided-wave signal processing methods (Li et al., 2009; Rafiee and Tse, 2009) that can be used for damage prognosis.

For the purpose of delamination damage detection with Lamb waves, it is necessary to understand the mechanism of interaction between Lamb waves and delamination damage. Numerical methods, for example, finite element (FE) method (Hosten and Castaignes, 2006; Ramadas et al., 2009, 2010), boundary element method (Cho and Rose, 1996), and spectral element method (Kudela et al., 2007), can help in understanding the mechanism of wave interaction with delamination.

College of Mechanical Engineering and Applied Electronics Technology,
Beijing University of Technology, Beijing, People's Republic of China

Corresponding author:

Zenghua Liu, College of Mechanical Engineering and Applied Electronics
Technology, Beijing University of Technology, Beijing, 100124, People's
Republic of China.
Email: liuzenghua@bjut.edu.cn

Guo and Cawley (1993) studied the interaction of Lamb wave mode S_0 with delamination located at various interfaces between the layers in an 8-ply cross-ply composite laminate $[(0/90)_2]_S$ by FE analysis. It was concluded that S_0 mode cannot interrogate the entire thickness of the laminate because the amplitude of the reflection of the S_0 mode from a delamination is strongly dependent on the position of the delamination through the thickness of the laminate, and no wave reflection takes place when shear stress is zero at that interface. Ramadas et al. (2009) studied the interaction of Lamb wave mode A_0 with symmetric delaminations in a quasi-isotropic laminated composite plate using two-dimensional (2D) FE model. It was found that when the A_0 mode interacts with a symmetric delamination, an S_0 mode could be generated and was confined only to sub-laminates. The research also shows that a converted A_0 mode will be generated and propagates in the main and sub-laminates because of the interaction of the newly generated S_0 mode with the delamination. Li et al. (2012) studied Lamb wave propagation in composite beam with delamination using a three-dimensional (3D) spectral element method. Research results show that the antisymmetric mode is more suitable for the identification of delamination in composite structures.

Lamb waves can be excited and detected by a variety of means. During manipulation, to ensure the efficient transfer of mechanical energy between the transducer and the test specimen, couplants are generally necessary. Couplants such as water, glycerin, and vaseline are often used in practice. However, materials may be degraded through absorption of these couplants. Air-coupled testing emerges as an alternative and promising method for noncontact testing. Electrostatic, air-coupled ultrasonic transducers were used for the first time in the 1970s for propagating waves in solids (Luukkala and Meriläinen, 1973). Noncontact air-coupled ultrasound is widely used for nondestructive testing in both metal and composite materials. Since polymer matrix composites have lower acoustic impedance than metals, air-coupled ultrasonic inspection for polymer matrix composites received considerable attention over the past decades (Castaings et al., 1998; Castaings and Hosten, 2001; Hosten et al., 1996; Kazys et al., 2006; Raisutis et al., 2011). More recently, the development of high-efficiency air-coupled ultrasonic transducers (Bhardwaj, 2009) and improvements in ultrasonic transmitting and receiving instruments (e.g. high-decibel preamplifier) make air-coupled ultrasonic

testing a powerful nondestructive method. These investigations showed that Lamb waves can be excited and detected using air-coupled ultrasonic transducers in composite plates with appropriate incident angle. Castaings and Cawley (1996) have shown that a pure Lamb mode can be excited with appropriate orientation of transmitting transducer, and A_0 mode is easy to be excited and detected because of its large out-of-plane surface displacement.

In this article, the interaction of Lamb wave mode A_0 with delamination is investigated with 3D FE models in the second section. The FE models of composite laminates with delaminations are created by a parametric modeling method using MATLAB scripts to generate input files for ABAQUS. The interactions between A_0 mode and delaminations with different lengths and located at different interfaces are investigated in detail. The experimental work with air-coupled ultrasonic transducers and signal processing technique are performed in the third section. In experimental study, one transducer is oriented at a special angle to generate a pure A_0 mode, and the other transducer is oriented to capture the reflected wave and transmitted wave. The location and size of delamination can be evaluated by extracting the time-of-flight (TOF) of reflected wave. Finally, conclusions are given in the fourth section.

FE simulation

The 3D FE simulations are carried out using MATLAB scripts to create input files for ABAQUS. The test specimens are 16-ply quasi-isotropic carbon fiber-reinforced epoxy composite beams with $[(0/45/90/-45)_2]_S$ layup. Each layer of these composite beams has a thickness of 0.14 mm. The material properties of these composite beam specimens are listed in Table 1. In the model, the dimensions of the composite beam are 400 mm (length) \times 30 mm (width) \times 2.24 mm (thickness), as shown in Figure 1.

In FE simulations, the composite beam model is meshed into 16 layers in thickness, and the material properties in each layer are assigned according to the layup of the composite beam. For the sake of simplicity, no damping is considered in the FE model. The type of element used for FE modeling is C3D8R, which is a linear, eight-node, 3D brick-type element. As the beam is meshed to 16 layers in thickness, the element size in thickness (z -direction) is 0.14 mm. The element sizes in length (x -direction) and in width (y -direction)

Table 1. Material properties of 16-ply carbon fiber-reinforced epoxy composite beam.

| E_1 (GPa) | E_2 (GPa) | E_3 (GPa) | G_{12} (GPa) | G_{13} (GPa) | G_{23} (GPa) | ν_{12} | ν_{13} | ν_{23} | ρ (kg/m ³) |
|-------------|-------------|-------------|----------------|----------------|----------------|------------|------------|------------|-----------------------------|
| 135 | 8.8 | 8.8 | 4.47 | 4.47 | 3.45 | 0.3 | 0.3 | 0.34 | 1560 |

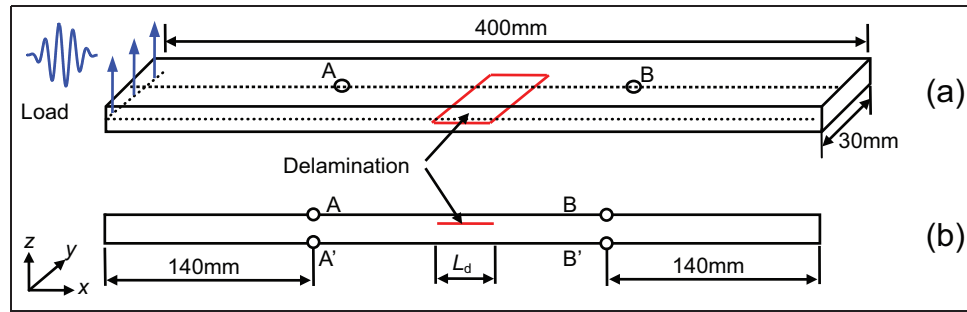


Figure 1. Composite beam model: (a) dimensions of the beam and (b) monitoring locations.

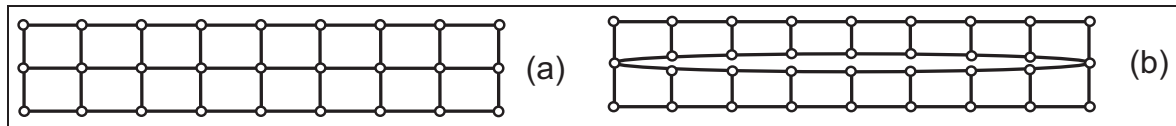


Figure 2. FE mesh of the composite beam model (a) with no delamination and (b) with delamination.
FE: finite element.

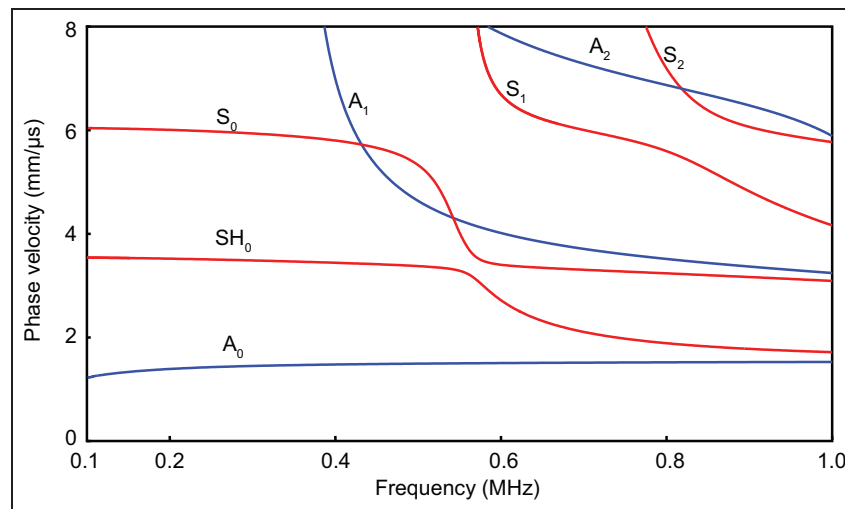


Figure 3. Dispersion curves of guided waves traveling along 0° direction in the composite beam.

are both 0.4 mm. An incremental time step of $0.02 \mu\text{s}$ is chosen in the FE models for this investigation. At the center frequency of 200 kHz, the group velocities of A_0 and S_0 modes are 1589 and 5910 m/s, respectively. The wavelength of A_0 mode at 200 kHz is 7.95 mm. The element and time step size are selected according to the convergence conditions proposed by Castaings and Cawley (1996). Through-width delamination with a length of L_d is modeled in the middle of the length of the beam as shown in Figure 1. FE mesh of composite beam is schematically illustrated in Figure 2 in 2D view. The delamination in the beam specimen is modeled by node separation. As illustrated in Figure 2(b), the nodes across the interface of delamination share the same coordinate values but have different node numbers,

attaching to adjacent elements. No contact mechanism between two surfaces of delamination is considered.

Dispersion curves of guided waves traveling along 0° direction in the composite beam are plotted in Figure 3. As shown in Figure 3, the number of coexistence of guided wave modes goes up as the frequency increases. The coexistence of many wave modes makes the signal analysis difficult. Besides, the attenuation coefficients of ultrasonic waves in air and composite materials increase as the excitation frequency increases. However, Lamb wave modes A_0 are more dispersive in the low frequency range. So, 200 kHz is chosen as the appropriate excitation center frequency to reach a good balance between mode complexity, attenuation, and dispersion. A five-cycle sinusoidal tone burst modulated by a

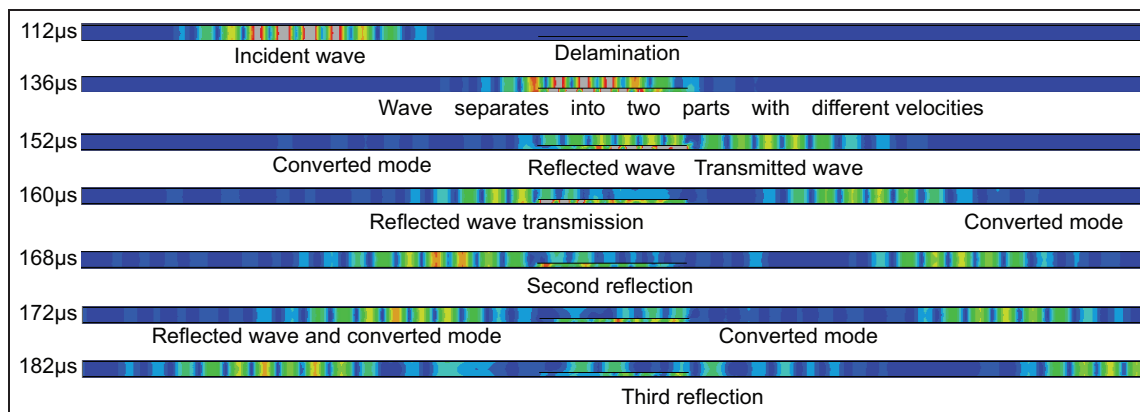


Figure 4. Snapshots of displacement fields at different time instants.

Hanning window with a central frequency of 200 kHz is chosen as the excitation signal. To excite a pure A_0 mode, a distributed force of the selected waveform is applied at the nodes on the middle of left end of composite beam, as schematically illustrated in Figure 1.

The interaction of Lamb waves with delaminations

A composite beam specimen with through-width delamination between the fourth and fifth layers is investigated first in this study. The length of the delamination, L_d , is 20 mm. The snapshots of the displacement fields at different time instants are presented in Figure 4.

The snapshot at 112 μs shows that the incident A_0 mode propagates in the main laminate. Incident wave separates into two parts with different velocities propagating in sub-laminates (delamination area), as shown in the snapshot at 136 μs. The snapshot at 152 μs shows that large reflection occurs when the wave in the sub-laminates propagates into the main laminate. The snapshot at 160 μs shows that considerable waves transmit across delamination and little converted mode advances the transmitted wave. Second transmission and reflection are seen in the snapshot at 168 μs when reflected wave in the sub-laminates propagates to the main laminate. The snapshot at 182 μs reveals that reflected waves transmit across the right end of delamination, and a part of waves again is reflected at the right end of delamination. It is concluded that large reflection and mode conversion will happen when Lamb waves propagate from the sub-laminates to main laminate.

To Lamb waves, the direction of particle displacement is mainly in-plane for symmetric wave modes and out-of-plane for antisymmetric wave modes (Rose, 1999). For the fundamental Lamb wave modes, A_0 mode has symmetric out-of-plane displacement and antisymmetric in-plane displacement, and meanwhile, S_0 mode has antisymmetric out-of-plane displacement and symmetric in-plane displacement. In FE models, time history of out-of-plane displacement and in-plane

displacement of monitoring nodes is recorded. By adding the out-of-plane displacements and in-plane displacements of the nodes at upper and lower surfaces, respectively, A_0 and S_0 modes can be individually extracted. For a intact beam and a beam with a delamination of 20 mm length between the fourth and fifth layers, A_0 mode at node A (A_{A_0}), S_0 mode at node A (A_{S_0}), A_0 mode at node B (B_{A_0}), and S_0 mode at node B (B_{S_0}) are extracted and plotted as shown in Figure 5. Due to the existence of delamination, reflection and mode conversion can be observed.

Wave propagation in the beams with delaminations with different lengths is further investigated. The delamination is still located at the interface between the fourth and fifth layers. The length of delamination increases from 5 to 60 mm with a step of 5 mm. A_0 and S_0 modes are extracted and are plotted as shown in Figure 6. For monitoring node A, reflected wave and converted mode delay in time domain as the delamination length L_d increases. It can be confirmed that large reflection and mode conversion take place when wave propagates from the sub-laminates to the main laminate. When the wave reflected from the right end of delamination propagates and reaches the left end of delamination, little reflected wave is also observed in monitoring node B.

Lamb wave propagation in composite beams with delaminations located at different interfaces

Wave propagation in composite beams with 20-mm-long delamination at different interfaces is investigated in this section. The delamination is located at the interfaces between the adjacent layers from the first to eighth layer, as labeled in Figure 7. Time histories of converted S_0 modes in composite beams are extracted and are plotted as shown in Figure 7. It is observed that there is little mode conversion in the composite beam with delamination between fourth and fifth layers and no mode conversion when delamination is located

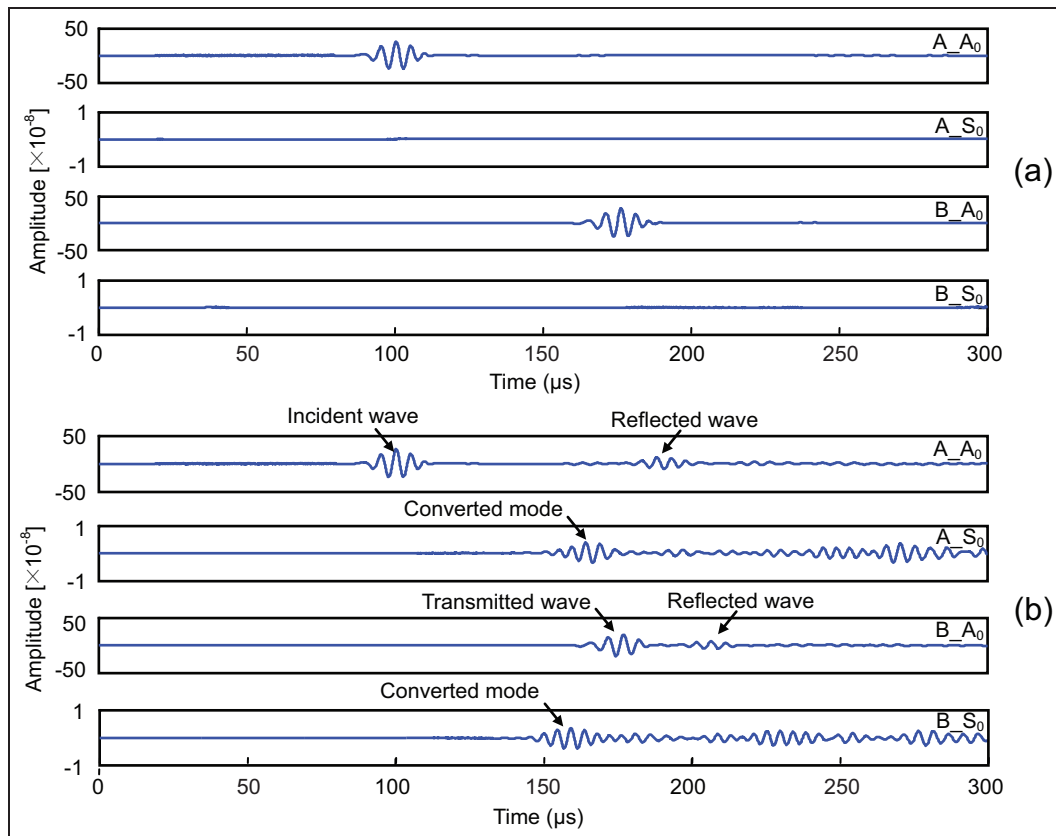


Figure 5. A_0 and S_0 modes in composite beams (a) with no delamination and (b) with the through-width delamination of 20 mm length.

between eighth and ninth layers. For this 16-layer composite beam with $[(0/45/90/-45)_2]_S$ layup, it is attributed to sub-symmetric or symmetric layup of the beam specimen.

Experimental work

Experimental setup

The experimental setup consists of a high-power ultrasonic measurement system RITEC RAM-5000 with a high-decibel preamplifier and a 50- Ω termination as its accessories, a personal computer (PC), an oscilloscope, and a scanning mechanism. The schematic diagram of the experimental setup is shown in Figure 8, where the RITECRAM-5000 is used to generate high-power tone burst voltages for the excitation of the transmitting transducer and to amplify received signal of the receiving transducer with its preamplifier. The PC is also used to control the scanning mechanism for transducer movement. In the scanning mechanism, a pair of transducer fixtures is used to hold and to orient the air-coupled ultrasonic transducers at a special angle for the excitation and collection of Lamb wave signals. The signals are collected by the oscilloscope. The air-coupled ultrasonic transducers employed in the

experiment are circular gas matrix piezoelectric composite transducers produced by the Ultrat Group (Model: NCG200-D13) with a diameter of 12.5 mm. The unfocused air-coupled transducers have a center frequency of 200 kHz, and bandwidth at -6 dB is 62 kHz. A five-cycle sinusoidal tone burst modulated by a Hanning window with a central frequency of 200 kHz is also applied on the transducer as the excitation signal. The transducer arrangement for delamination detection is illustrated in Figure 9. To excite a pure Lamb wave A_0 mode along 0° direction of composite beam, the transmitting transducer is adjusted to 14° based on Snell's law (Castaings and Cawley, 1996).

Delamination inspection

The test specimens used here are carbon fiber-reinforced epoxy composite beams with the same thickness, width, material properties, and layup as those used in FE analysis. The dimensions of the composite beam specimens are 800 mm (length) \times 30 mm (width) \times 2.24 mm (thickness). Dispersion curves of guided waves traveling along 0° direction in the composite beam are plotted in Figure 3. Through-width delamination is introduced by inserting Teflon film (0.05 mm in thickness) between the fourth and fifth layers during

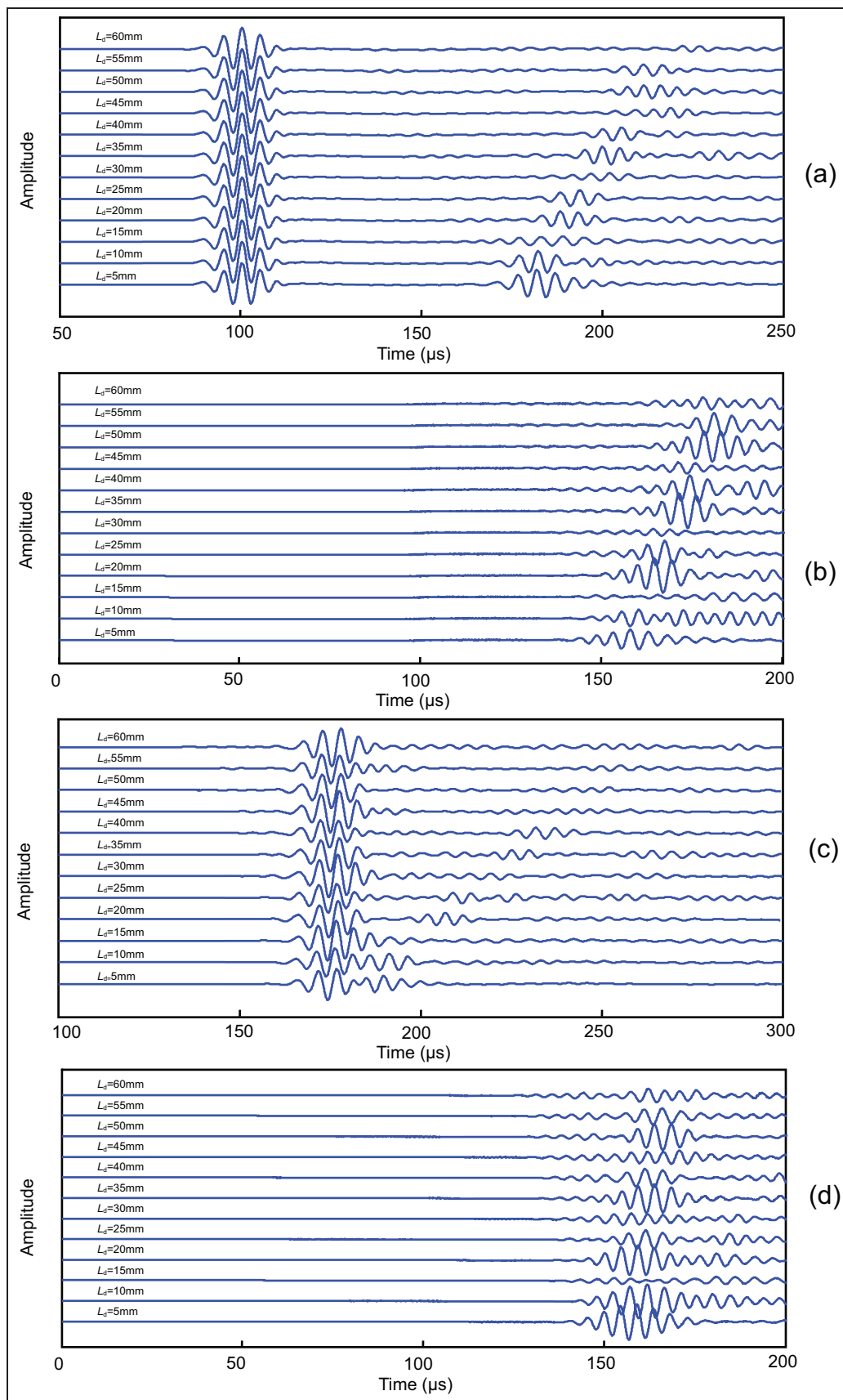


Figure 6. Incident mode and converted mode in composite beams with delamination located at the interface between the fourth and fifth layers: (a) A_{A_0} , (b) A_{S_0} , (c) B_{A_0} , and (d) B_{S_0} .

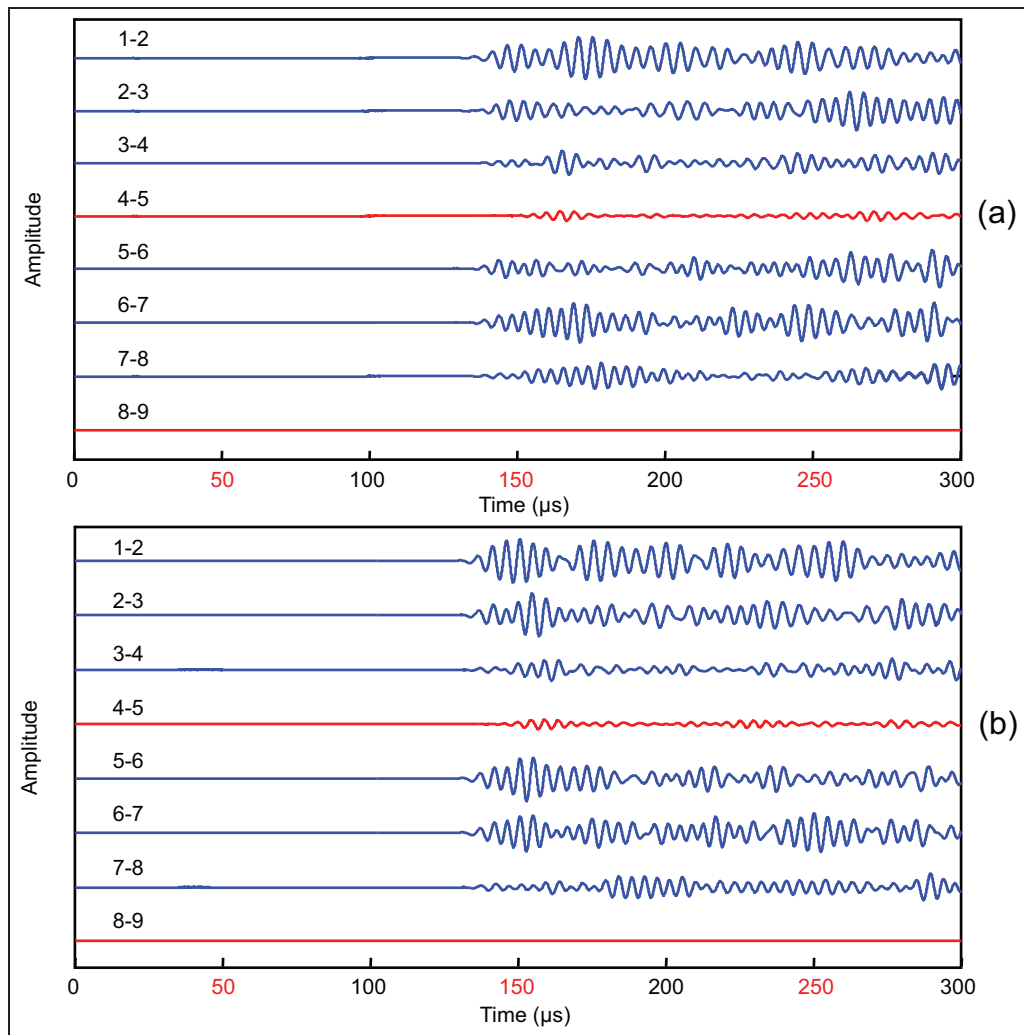


Figure 7. Converted S_0 modes in composite beams with delaminations located at different interfaces: (a) A_{S_0} and (b) B_{S_0} .

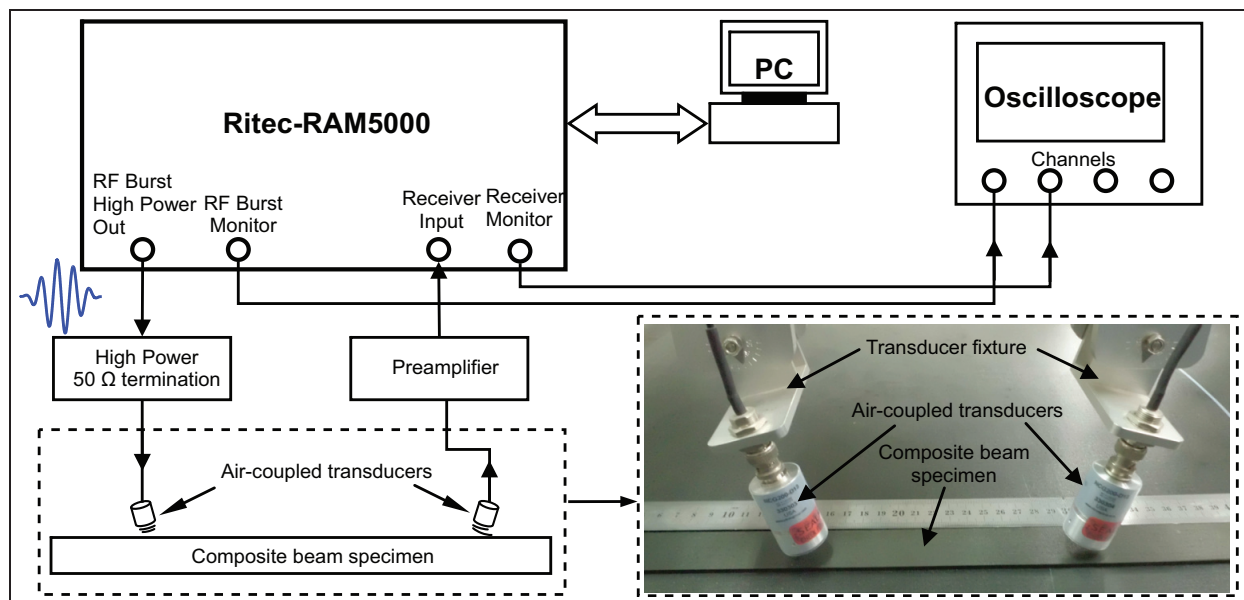


Figure 8. Schematic diagram of the experimental setup.

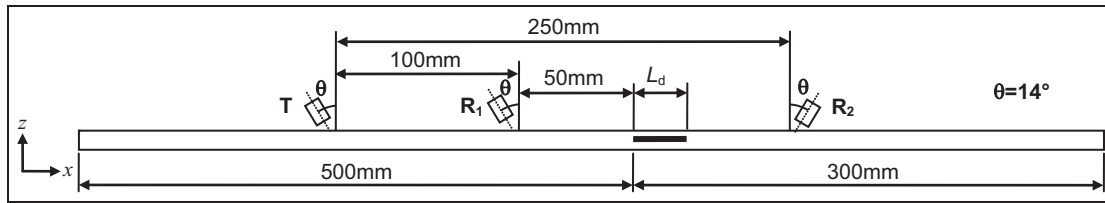


Figure 9. Transducer arrangement for delamination detection in carbon fiber-reinforced epoxy composite beam.

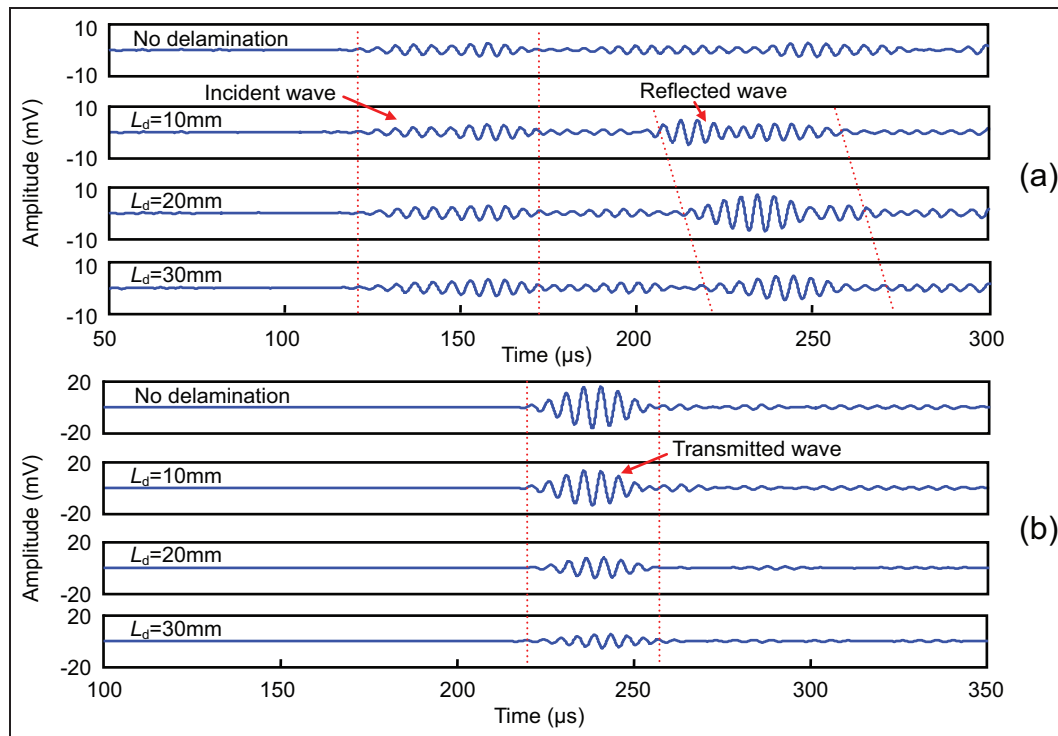


Figure 10. Received Lamb wave signals in composite beams with different L_d by using (a) R_1 and (b) R_2 transducers.

the layup procedure. The length of delamination L_d is 10, 20, and 30 mm. As illustrated in Figure 9, one air-coupled receiving transducer R_1 is oriented in the same direction as the transmitting transducer and another air-coupled receiving transducer R_2 is oriented in contrast to that transmitting transducer. Dobie et al. (2011) discovered that the receiving transducer with the same orientation as transmitting transducer mainly captures the reflected wave and the transducer oriented in contrast to that transmitting transducer mainly captures the direct incident wave. For the transducer arrangement illustrated in Figure 9, receiving transducer R_1 will mainly capture wave propagating in -0° direction (reflected wave) and receiving transducer R_2 will mainly capture wave propagating in 0° direction (transmitted wave).

For composite beams with different lengths of delamination, received Lamb wave signals by using R_1 and R_2 transducers are plotted in Figure 10. Due to orientation of transducer R_1 , the amplitude of reflected wave

is even larger than the incident wave. This reflected wave is proven as reflection at the right end of delamination by time delay of wave packages as L_d increases. Therefore, the location of the right end of delamination can be evaluated using the TOF and the group velocity of the reflected wave. Similarly, the left end of delamination can also be evaluated if the excitation is located at the right end of the composite beam. Therefore, the location and size of the delamination can be evaluated quantitatively. Phase change is also observed after waves propagating across the delamination. The amplitude of transmitted wave decreases as L_d increases.

Conclusion

The interaction of Lamb wave A_0 mode with delamination in laminated composite beams is investigated in detail through 3D FE simulation. It is concluded that large reflection and mode conversion will happen when

Lamb waves propagate from the sub-laminates to main laminate. It is also observed that there is little or no converted S_0 mode when A_0 mode encounters delamination located at sub-symmetric interface and symmetric interface. In experimental study, noncontact air-coupled transmitting transducer is oriented at a coincidence angle so that a pure A_0 mode can be excited. Results show that a pure A_0 mode can be effectively excited and detected using air-coupled ultrasonic transducers. It is also observed that air-coupled receiving transducer oriented in the same direction as transmitting transducer will mainly capture reflected wave and air-coupled receiving transducer oriented in contrast to that transmitting transducer will mainly capture the transmitted wave. Through-width delamination can be located and sized by capturing reflected waves at both ends of delamination.

Funding

This work was supported by National Natural Science Foundation of China (nos 11272021 and 50975006), Beijing Natural Science Foundation (no. 1122007), General Program of Science and Technology Development Project of Beijing Municipal Commission of Education (no. KM201010005003), the Importation and Development of High-Caliber Talents Project of Beijing Municipal Institutions (no CIT&TCD201304048), and Beijing Nova Program (no. 2008A015).

References

- Bhardwaj MC (2009) Phenomenally high transduction air/gas transducers for practical non-contact ultrasonic applications. In: *AIP conference proceedings, review of progress in quantitative nondestructive evaluation* (eds D Thompson and DE Chimenti), Chicago, IL, 20–25 July, vol. 1096, pp. 920–927. College Park, MD: AIP.
- Castaings M and Cawley P (1996) The generation, propagation and detection of Lamb waves in plates using air-coupled ultrasonic transducers. *Journal of the Acoustical Society of America* 100(5): 3070–3077.
- Castaings M and Hosten B (2001) Lamb and SH waves generated and detected by air-coupled ultrasonic transducers in composite material plates. *NDT & E International* 34(4): 249–258.
- Castaings M, Cawley P, Farlow R, et al. (1998) Single sided inspection of composite materials using air coupled ultrasound. *Journal of Nondestructive Evaluation* 17(1): 37–45.
- Cawley P and Alleyne D (1996) The use of Lamb waves for the long range inspection of large structures. *Ultrasonics* 34(2–5): 287–290.
- Cho YH and Rose JL (1996) A boundary element solution for a mode conversion study on the edge reflection of Lamb waves. *Journal of the Acoustical Society of America* 99(4): 2097–2109.
- Dobie G, Spencer A, Burnham K, et al. (2011) Simulation of ultrasonic lamb wave generation, propagation and detection for a reconfigurable air coupled scanner. *Ultrasonics* 51(3): 258–269.
- Farrar CR and Lieven NAJ (2007) Damage prognosis: the future of structural health monitoring. *Philosophical Transactions of the Royal Society A: Mathematical Physical and Engineering Sciences* 365(1851): 623–632.
- Giurgiutiu V (2005) Tuned Lamb wave excitation and detection with piezoelectric wafer active sensors for structural health monitoring. *Journal of Intelligent Material Systems and Structures* 16(4): 291–305.
- Guo N and Cawley P (1993) The interaction of Lamb waves with delaminations in composite laminates. *Journal of the Acoustical Society of America* 94(4): 2240–2246.
- Guo N and Cawley P (1994) Lamb wave reflection for the quick nondestructive evaluation of large composite laminates. *Materials Evaluation* 52(3): 404–411.
- Hosten B and Castaings M (2006) FE modeling of Lamb mode diffraction by defects in anisotropic viscoelastic plates. *NDT & E International* 39(3): 195–204.
- Hosten B, Hutchins DA and Schindel DW (1996) Measurement of elastic constants in composite materials using air-coupled ultrasonic bulk waves. *Journal of the Acoustical Society of America* 99(4): 2116–2123.
- Islam AS and Craig KC (1994) Damage detection in composite structures using piezoelectric materials. *Smart Materials and Structures* 3(3): 318–328.
- Kazys R, Demcenko A, Zukauskas E, et al. (2006) Air-coupled ultrasonic investigation of multi-layered composite materials. *Ultrasonics* 44(Suppl.): e819–e822.
- Kudela P, Zak A, Krawczuk M, et al. (2007) Modelling of wave propagation in composite plates using the time domain spectral element method. *Journal of Sound and Vibration* 302(4–5): 728–745.
- Lee JS, Park G, Kim CG, et al. (2011) Use of relative baseline features of guided waves for in situ structural health monitoring. *Journal of Intelligent Material Systems and Structures* 22(2): 175–189.
- Li FC, Meng G, Kageyama K, et al. (2009) Optimal mother wavelet selection for Lamb wave analyses. *Journal of Intelligent Material Systems and Structures* 22(10): 1147–1161.
- Li FC, Peng HK, Sun XW, et al. (2012) Wave propagation analysis in composite laminates containing a delamination using a three-dimensional spectral element method. *Mathematical Problems in Engineering* 2012: 659849 (19 pp.).
- Luukkala M and Meriläinen P (1973) Metal plate testing using airborne ultrasound. *Ultrasonics* 11(5): 218–221.
- Mascarenas DDL, Flynn EB, Todd MD, et al. (2010) Development of capacitance-based and impedance-based wireless sensors and sensor nodes for structural health monitoring applications. *Journal of Sound and Vibration* 329(12): 2410–2420.
- Park G, Sohn H, Farrar CR, et al. (2003) Overview of piezoelectric impedance-based health monitoring and path forward. *Shock and Vibration Digest* 35(6): 451–463.
- Rafiee J and Tse PW (2009) Use of autocorrelation of wavelet coefficients for fault diagnosis. *Mechanical Systems and Signal Processing* 23(5): 1554–1572.
- Raisutis R, Kazys R, Zukauskas E, et al. (2011) Ultrasonic air-coupled testing of square-shape CFRP composite rods by means of guided waves. *NDT & E International* 44(7): 645–654.
- Ramadas C, Balasubramaniam K, Joshi M, et al. (2009) Interaction of the primary anti-symmetric Lamb mode (A_0) with symmetric delaminations: numerical and

- experimental studies. *Smart Materials and Structures* 18(8): 085011 (7 pp.).
- Ramadas C, Balasubramaniam K, Joshi M, et al. (2010) Interaction of guided Lamb waves with an asymmetrically located delamination in a laminated composite plate. *Smart Materials and Structures* 19(6): 065009 (11 pp.).
- Rizzo P, Han JG and Ni XL (2010) Structural health monitoring of immersed structures by means of guided ultrasonic waves. *Journal of Intelligent Material Systems and Structures* 21(14): 1397–1407.
- Rose JL (1999) *Ultrasonic Waves in Solid Media*. New York: Cambridge University Press.
- Su ZQ, Ye L and Lu Y (2006) Guided Lamb waves for identification of damage in composite structures: a review. *Journal of Sound and Vibration* 295(3–5): 753–780.
- Wilcox PD, Lowe MJS and Cawley P (2001) Mode and transducer selection for long range Lamb wave inspection. *Journal of Intelligent Material Systems and Structures* 12(8): 553–565.